Incentive-based Coordinated Charging Control of Plug-in Electric Vehicles at the Distribution-Transformer Level

Ralph Hermans, *Student Member* Mads Almassalkhi, *Student Member* Ian Hiskens, *Fellow*

***Abstract*— Distribution utilities are becoming increasingly aware that their networks may struggle to accommodate large numbers of plug-in electric vehicles (PEVs). In particular, uncoordinated overnight charging is expected to be problematic, as the corresponding aggregated power demand exceeds the capacity of most distribution substation transformers. In this paper, a dynamical model of PEVs served by a single temperature-constrained substation transformer is presented and a centralized scheduling scheme is formulated to coordinate charging of a heterogeneous PEV fleet. We employ the dual-ascent method to derive an iterative, incentive-based and non-centralized implementation of the PEV charging algorithm, which is optimal upon convergence. Then, the distributed open-loop problem is embedded in a predictive control scheme to introduce robustness against disturbances. Simulations of an overnight charging scenario illustrate the effectiveness of the so-obtained incentive-based coordinated PEV control scheme in terms of performance and enforcing the transformer's thermal constraint.**

I. Introduction

As gasoline prices increase and concerns regarding greenhouse gas emissions grow, plug-in electric vehicles (PEV) become an appealing alternative to the traditional internal-combustion-based automobiles that prevail today. PEVs are therefore expected to gain a significant market share over the next couple of decades.

However, while PEV sales are already on the rise today, distribution utilities are becoming increasingly aware that their networks may struggle to accommodate large levels of plug-in penetration [1]. In particular, *en masse* uncoordinated charging at night is deemed to be problematic, as the corresponding power demand exceeds the capacity of most distribution substation transformers [2]. Persistent overloading of such transformers may cause insulation breakdown, resulting ultimately in transformer failure and blackout of the full residential area that it serves.

Network upgrades are a trivial but expensive solution to the above issue. The need for investments may be alleviated considerably by coordinating PEV charging in such a way that network restrictions are respected at all times. The implementation of such control schemes is facilitated by modern communication technologies that allow for monitoring and maneuvering of individual electrical loads.

Some of the first PEV-load schemes provided by the literature rely on centralized open-loop scheduling and direct manipulation of PEV charging rates by the network utilities, see [3]–[5]. Such approaches typically suffer from a significant need for communication and excessive computational burdens, however. Other work on PEV scheduling focuses on hierarchical control as a possible means of decreasing complexity [6]. Therein, the distribution-level transformers are treated as static network elements with a given power rating (i.e., a fixed capacity) and the dynamical relationship between transformer loading and winding temperature is ignored. However, perhaps even more problematic than the associated computational complexity, utility-controlled charging may be impractical as PEV owners could be reluctant to relinquish the control of their vehicles to some centralized operator, and they might be unwilling to cooperate with each other if this could affect their own charging performance.

In recent work, see [7], [8], PEV owners are therefore considered to be autonomous entities whose actions can only be influenced by providing them with incentives (i.e., a time-varying electricity price) for a certain behavior. A key assumption in [7] is that the PEVs are price takers: individually, their strategies have no significant effect on the aggregate power demand and price. The so-obtained coordinated scheduling scheme lets each vehicle effectively react to the average charging strategy of the total (infinitely large) PEV population and establishes a Nash-optimal, valley-filling net charging profile by encouraging additional charging whenever background demand is low. While [8] achieves the valley-filling effect with any number of PEVs, both [7] and [8] employ utility-centric objectives that essentially sacrifice PEV-owner convenience and access to grid to ensure that the network capacity is minimally utilized at all times.

In contrast to [7], [8], our interests align with incentive-based PEV charging control at the *distribution-transformer level*, which is characterized by a relatively small vehicle population (20–50 PEVs). As a consequence, it is possible for each PEV to affect the aggregate demand considerably and the price-taking and utility-centric assumptions of [7], [8] do not hold. Thus, instead of the valley-filling charging strategy, a different control strategy must be pursued.

In this paper, we formulate a centralized open-loop predictive optimization problem that, in contrast to the methods proposed in [6]–[8], explicitly accounts for the transformer's thermal limit and dynamics when computing the control actions. Moreover, because prediction errors and fluctuations

This work was supported by the U.S. Department of Energy under research grant DE-SC0002283, the US-China CERC for Clean Vehicle Collaboration, and the EOS-LT Regelduurzaam project funded by the Dutch Ministry of Economic Affairs.

Mads Almassalkhi and Ian Hiskens are with the Department of Electrical Engineering and Computer Science, University of Michigan, 1301 Beal Avenue, Ann Arbor, MI 48109, U.S.A. E-mails: {malmassa, hiskens}@umich.edu.

Ralph Hermans is with the Department of Electrical Engineering: Control Systems, Eindhoven University of Technology, P.O. Box 513, 5600 MB Eindhoven, The Netherlands. E-mail: r.m.hermans@tue.nl.

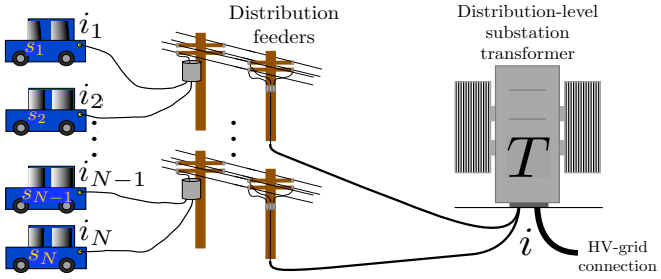

Fig. 1. PEV charging via a single substation transformer.

in background demand can be severe due to a low extent of aggregation in the distribution network, we introduce feedback to disturbances by solving the scheduling problem in a receding horizon fashion. The resulting centralized *model predictive control* (MPC) scheme is then decomposed into a set of local control laws, which determine the charging strategy of each individual electric vehicle, and which are coordinated via a common (pseudo-)price for electrical energy. This price is generated by a centralized agent in such a way that aggregated power demand is kept within operational limits while PEVs are allowed to charge as quickly as possible. Simulation results are provided to demonstrate the effectiveness of the distributed approach and to allow for comparison with existing PEV charging schemes. We end with conclusions and recommendations for further research.

A. Basic notation and definitions

Let $\mathbb{R}$, $\mathbb{R}_+$, $\mathbb{Z}$ and $\mathbb{Z}_+$ denote the sets of reals, non-negative reals, integers and non-negative integers, respectively. For each $c \in \mathbb{R}$ and $\Pi \subseteq \mathbb{R}$ let $\Pi_{\geq c} := \{k \in \Pi \mid k \geq c\}$ and similarly, $\Pi_{\leq c}$. Let $\mathbb{Z}_\Pi := \mathbb{Z} \cap \Pi$. For a finite set $\{x_i\}_{i\in\mathbb{Z}_{[1,N]}}$, $x_i \in \mathbb{R}^{n_i}$, $N \in \mathbb{Z}_{\geq 1}$, let $\mathrm{col}(\{x_i\}_{i\in\mathbb{Z}_{[1,N]}})$ and $\mathrm{col}(x_1, \ldots, x_N)$ denote the vector $\left(x_1^\top, \ldots, x_N^\top\right)^\top$. Let $\mathbf{1}_n$ be the all-one vector $\left[\begin{smallmatrix}1 & \ldots & 1\end{smallmatrix}\right]^\top$ in $\mathbb{R}^n$, and $\mathbf{I}_n$ the n by n identity matrix. The i-th element of a vector $x \in \mathbb{R}^n$ is denoted by $[x]_i$. Define projection $[x]_+ \in \mathbb{R}^n_+$ by $[[x]_+]_i := \max\{0, [x]_i\}$. Let $\mathbf{z} := \{z(l)\}_{l\in\mathbb{Z}_+}$ with $z(l) \in \mathbb{R}^n$, $l \in \mathbb{Z}_+$, denote an arbitrary sequence. For some scalar $c \in \mathbb{R}$, let $\lceil c \rceil := \min_{k\in\mathbb{Z}_{\geq c}} k$ and let $|c|$ be its absolute value. All inequalities are interpreted elementwise.

II. Dynamical Model

We begin by describing a model for the PEV charging problem. Consider a fleet of $N \in \mathbb{Z}_+$ plug-in electric vehicles, all connected to a distribution grid that is fed by a single substation transformer, see Fig. 1. Let the continuous-time charging dynamics of vehicle $n \in \mathcal{N} := \{1, \ldots, N\}$ be described by

$$\dot{s}_n(t) = \tilde{\eta}_n p_n(t) = \tilde{\eta} V_{\mathrm{AC}} i_n(t), \qquad t \in \mathbb{R}_+, \tag{1}$$

where $s_n(t)$, $p_n(t)$ [W] and $i_n(t)$ [A] denote the vehicle battery's normalized state of charge (SOC), the charging power and the charging current at continuous-time instant $t \in \mathbb{R}_+$, respectively. We assume that the rms grid voltage V_{AC} [V] is constant. The parameter $\tilde{\eta}_n$ [J^{-1}] is obtained as the ratio of the vehicle's charging efficiency $\alpha_n \in \mathbb{R}_{[0,1]}$ and battery size β_n [J]. Note that the above dynamics are valid only for s_n in $\mathbb{R}_{[0,1]}$, where $s_n = 1$ and $s_n = 0$ mean that the battery of vehicle $n \in \mathcal{N}$ is fully charged and empty, respectively. Next, suppose that the charging profiles $i_n(t)$ are step-wise with step width T_s [s], such that $i_n(t) := i_n[k]$ for $t \in \mathbb{R}_{[kT_\mathrm{s},(k+1)T_\mathrm{s})}$ and $k \in \mathbb{Z}_+$. Then, (1) yields

$$s_n[k+1] = s_n[k] + \eta_n i_n[k], \qquad k \in \mathbb{Z}_+, \tag{2}$$

where $s_n[k] := s_n(kT_\mathrm{s})$ and $\eta_n := T_\mathrm{s}\tilde{\eta}_n V_{\mathrm{AC}}$ [A^{-1}].

The transformer that connects the distribution grid to the high-voltage transmission network is modeled as a single thermal mass with continuous-time temperature dynamics

$$\dot{T}(t) = \frac{1}{C}\left\{R_\mathrm{c} i^2(t) - \frac{T(t) - T_\mathrm{a}(t)}{R}\right\}, \tag{3}$$

with aggregated current $i(t) := i_\mathrm{d}(t) + \sum_{n\in\mathcal{N}} i_n(t)$ [A], transformer heat capacity C [$\mathrm{J\ K}^{-1}$], heat outflow resistance R [$\mathrm{K\ W}^{-1}$], coil resistance R_c [Ω], and where $T(t)$ [K] is the transformer core temperature at time instant $t \in \mathbb{R}_+$. The net background/non-PEV current $i_\mathrm{d}(t)$ [A] and the ambient temperature $T_\mathrm{a}(t)$ [K] act as exogenous disturbances. Using Euler forward discretization and sampling period T_s, the following discrete-time temperature model is obtained:

$$T[k+1] = \tau T[k] + \bar{\gamma} i^2[k] + \rho T_\mathrm{a}[k], \tag{4}$$

where $\tau := \left(1 - \frac{T_\mathrm{s}}{RC}\right) \in \mathbb{R}$, $\bar{\gamma} := \frac{T_\mathrm{s} R_\mathrm{c}}{C} \in \mathbb{R}_+$ and $\rho := \frac{T_\mathrm{s}}{RC} = 1 - \tau \in \mathbb{R}_+$, and where $T[k]$ is the transformer core temperature at discrete-time instant $k \in \mathbb{Z}_+$. For stability, the sampling period is required to satisfy $0 < T_\mathrm{s} < 2RC$, such that $\tau \in \mathbb{R}_{(-1,1)}$.

In what follows, we use a linearized version of (4) to allow for a tractable implementation of the charging control scheme described in Sect. III. Linearization around the equilibrium point T^*, $i^* := \sqrt{\bar{\gamma}^{-1}\rho(T^* - T_\mathrm{a}^*)}$ for $T_\mathrm{a} := T_\mathrm{a}^*$ and $i_\mathrm{d} := 0$ yields the approximate transformer dynamics described by

$$\Delta T[k+1] = \tau \Delta T[k] + \gamma\left(i_\mathrm{d}[k] + \sum_{n\in\mathcal{N}} \Delta i_n[k]\right) + \rho \Delta T_\mathrm{a}[k], \tag{5}$$

with $\Delta T[k] := T[k] - T^*$, $\Delta i_n[k] := i_n[k] - \frac{i^*}{N}$ and $\Delta T_\mathrm{a}[k] := T_\mathrm{a}[k] - T_\mathrm{a}^*$, and where $\gamma := 2\bar{\gamma} i^*$.

Next, let $\{s_n[l \mid k]\}_{l\in\mathbb{Z}_{[0,K]}}$ and $\{\Delta T[l \mid k]\}_{l\in\mathbb{Z}_{[0,K]}}$ be the SOC and temperature sequences generated by (2) and (5) from initial state $\left[\begin{smallmatrix}s_1[k] & \ldots & s_N[k] & \Delta T[k]\end{smallmatrix}\right]^\top \in \left(\mathbb{R}_{[0,1]}\right)^N \times \mathbb{R}$, charging rate sequences $\{\Delta i_n[l \mid k]\}_{l\in\mathbb{Z}_{[0,K-1]}}$, $n \in \mathcal{N}$, and disturbances $\{i_d[l \mid k]\}_{l\in\mathbb{Z}_{[0,K-1]}}$, $\{\Delta T_\mathrm{a}[l \mid k]\}_{l\in\mathbb{Z}_{[0,K-1]}}$ over a finite prediction horizon $K \in \mathbb{Z}_+$. Next, consider the following sequence vector notation, i.e.,

$$\begin{aligned}
\mathbf{T}[k] &= \mathrm{col}\left(\{\Delta T[l \mid k]\}_{l\in\mathbb{Z}_{[0,K]}}\right) \in \mathbb{R}^{K+1} \\
\mathbf{s}_n[k] &= \mathrm{col}\left(\{s_n[l \mid k]\}_{l\in\mathbb{Z}_{[0,K]}}\right) \in \mathbb{R}^{K+1}, \qquad n \in \mathcal{N}, \\
\mathbf{d}[k] &= \mathrm{col}\left(\{d[l \mid k]\}_{l\in\mathbb{Z}_{[0,K-1]}}\right) \\
&:= \mathrm{col}\left(\left\{\left[\begin{smallmatrix} i_d[l|k] \\ \Delta T_\mathrm{a}[l|k]\end{smallmatrix}\right]\right\}_{l\in\mathbb{Z}_{[0,K-1]}}\right) \in \mathbb{R}^{2K} \\
\boldsymbol{\pi}_n[k] &= \mathrm{col}\left(\{\pi_n[l \mid k]\}_{l\in\mathbb{Z}_{[0,K-1]}}\right) \\
&:= \mathrm{col}\left(\{\Delta i_n[l \mid k]\}_{l\in\mathbb{Z}_{[0,K-1]}}\right) \in \mathbb{R}^{K}, \quad n \in \mathcal{N},
\end{aligned}$$

and the sequence vector of aggregated charging current

$$\boldsymbol{\pi}[k] = \operatorname{col}\left(\{\pi[l \mid k]\}_{l\in\mathbb{Z}_{[0,K-1]}}\right) := \textstyle\sum_{n\in\mathcal{N}} \boldsymbol{\pi}_n[k] \in \mathbb{R}^K,$$

such that (2) and (5) yield the prediction model

$$\mathbf{T}[k] = \boldsymbol{\Phi}\Delta T[k] + \boldsymbol{\Psi}\boldsymbol{\pi}[k] + \boldsymbol{\Psi}_{\mathrm{d}}\mathbf{d}[k] \tag{6}$$

$$\mathbf{s}_n[k] = \boldsymbol{\Phi}_{\mathrm{s}} s_n[k] + \boldsymbol{\Psi}_{S_n}\boldsymbol{\pi}_n[k], \qquad n \in \mathcal{N}, \tag{7}$$

with transition matrices $\boldsymbol{\Phi} \in \mathbb{R}^{K+1}$, $\boldsymbol{\Psi} \in \mathbb{R}^{(K+1)\times K}$, $\boldsymbol{\Psi}_{\mathrm{d}} \in \mathbb{R}^{(K+1)\times(2K)}$, $\boldsymbol{\Phi}_{\mathrm{s}} \in \mathbb{R}^{K+1}$, $\boldsymbol{\Psi}_{S_n} \in \mathbb{R}^{(K+1)\times K}$.

III. Centralized Scheduling of PEV Demand

Next, we formulate a centralized load scheduling strategy that serves as a starting point for the incentive-based, distributed control scheme derived in Sect. IV.

We begin by observing that, for safety or performance reasons, PEV battery charging is subject to strict state and input constraints. Firstly, battery chargers usually come with a limited power capacity, i.e.,

$$\pi_{n,\min} \le \pi_n[k] \le \pi_{n,\max}, \qquad k \in \mathbb{Z}_+, n \in \mathcal{N}, \tag{8}$$

with finite $\pi_{n,\min} \in \mathbb{R}$, $\pi_{n,\max} \in \mathbb{R}_+$. Note that vehicle-to-grid technology, which enables power delivery to the network, can be taken into consideration via negative $\pi_{n,\min}$.

Secondly, to prevent transformer overheating, a (relative) temperature constraint is imposed, i.e.,

$$T^* + \Delta T[k] \le T_{\max}, \qquad k \in \mathbb{Z}_+. \tag{9}$$

For simplicity, we restrict our attention to a static upper bound on temperature, even though this may be overly strict in practice. Normally, a slight temporary violation of (9) is allowed, provided that secure steady-state operating conditions are recovered within a sufficiently short subsequent cooling-down period.

Thirdly, by construction, the SOCs are bounded by

$$0 \le s_n[k] \le 1, \qquad k \in \mathbb{Z}_+. \tag{10}$$

Additionally, each PEV owner can set a certain SOC target that needs to be reached by the time they expect to leave their home. Thus, given (7) and initial states of charge $s_1[0], \dots, s_N[0]$, the load scheduling scheme has to select, for all $n \in \mathcal{N}$, an appropriate charging profile $\boldsymbol{\pi}_n[k]$ such that a certain minimum battery state $S_n \in \mathbb{R}_{[0,1]}$ is attained at some discrete-time instant $K_n \in \mathbb{Z}_{\le K}$. That is,

$$S_n \le s_n[k], \qquad k \in \mathbb{Z}_{\ge K_n}. \tag{11}$$

Next, recall that the individual charging rates $\pi_n[k]$ are coupled to temperature dynamics (6) and constraint (9) through the relation

$$\pi[k] = \textstyle\sum_{n\in\mathcal{N}} \pi_n[k], \qquad k \in \mathbb{Z}_+. \tag{12}$$

The set of solutions $\{\boldsymbol{\pi}_n\}_{n\in\mathcal{N}}$ to (6)–(12) given $\Delta T[k]$, $\{s_n[k]\}_{n\in\mathcal{N}}$ and $\mathbf{d}[k]$ is the set of valid charging/feasible control strategies. Note that this set is polytopic (and thus convex), as all constraints (6)–(12) are affine in $\boldsymbol{\pi}_n$.

The selection of a particular control schedule out of the set of feasible strategies may be based on an optimization criterion. In this paper, a PEV-centric objective is employed, namely, the minimization of SOC deviations from 1 and minimization of local battery wear and control effort. Thus, the centralized controller's composite objective is

$$\min_{\boldsymbol{\pi}_n[k],\mathbf{s}_n[k],n\in\mathcal{N}} \textstyle\sum_{n\in\mathcal{N}} J_n(\boldsymbol{\pi}_n[k], \mathbf{s}_n[k]) \tag{13}$$

where $J_n : \mathbb{R}^K \times \mathbb{R}^{K+1} \to \mathbb{R}_+$, $n \in \mathcal{N}$, is defined as

$$J_n(\boldsymbol{\pi}_n, \mathbf{s}_n) := \boldsymbol{\pi}_n^\top \mathcal{R}_n \boldsymbol{\pi}_n + (\mathbf{s}_n - \mathbf{1}_{K+1})^\top \mathcal{Q}_{s,n}(\mathbf{s}_n - \mathbf{1}_{K+1}),$$

with $\mathcal{Q}_{s,n} = Q_{s,n}\mathbf{I}_{K+1}$ and $\mathcal{R}_n = R_n\mathbf{I}_K$, for some $Q_{s,n}, R_n \in \mathbb{R}_{>0}$. Since both $Q_{s,n}$ and R_n are strictly positive and constraints (6)–(12) are linear, the optimization problem obtained by solving (13) over the set of feasible control strategies is strictly convex and any optimal solution is therefore globally optimal.

Now consider the following optimization problem.

Problem III.1 (Open-loop Centralized PEV Charging) Given $s_n[0 \mid k] = s_n[k]$ for $n \in \mathcal{N}$, $\Delta T[0 \mid k] = \Delta T[k]$ and disturbance forecast $\hat{\mathbf{d}}[k] := \operatorname{col}\left(\{\hat{d}[l \mid k]\}_{l\in\mathbb{Z}_{[0,K-1]}}\right)$, solve

$$\min_{\boldsymbol{\pi}_n,\, n\in\mathcal{N}} \sum_{n\in\mathcal{N}} \Big(\boldsymbol{\pi}_n^\top (\boldsymbol{\Psi}_{S_n}^\top \mathcal{Q}_{s,n} \boldsymbol{\Psi}_{S_n} + \mathcal{R}_n)\boldsymbol{\pi}_n \tag{14a}$$

$$+ 2(\boldsymbol{\Phi}_{S_n}\mathbf{s}_n[0 \mid k] - \mathbf{1}_{K+1})^\top \mathcal{Q}_{s,n}\boldsymbol{\Psi}_{S_n}\boldsymbol{\pi}_n \Big)$$

$$\text{s.t. } \boldsymbol{\Phi}\Delta T[0 \mid k] + \boldsymbol{\Psi}\left(\sum_{n\in\mathcal{N}} \boldsymbol{\pi}_n\right) + \boldsymbol{\Psi}_{\mathrm{d}}\hat{\mathbf{d}} \le T_{\max}\mathbf{1}_{K+1} \tag{14b}$$

$$\pi_{n,\min}\mathbf{1}_K \le \boldsymbol{\pi}_n \le \pi_{n,\max}\mathbf{1}_K \tag{14c}$$

$$0 \le \boldsymbol{\Phi}_{S_n} s_n[0 \mid k] + \boldsymbol{\Psi}_{S_n}\boldsymbol{\pi}_n \le \mathbf{1}_{K+1} \tag{14d}$$

$$S_n\mathbf{1}_{K-K_n+1} \le \mathbf{M}_{K_n}\left(\boldsymbol{\Phi}_{S_n} s_n[0 \mid k] + \boldsymbol{\Psi}_{S_n}\boldsymbol{\pi}_n\right) \tag{14e}$$

for all $n \in \mathcal{N}$, where $\mathbf{M}_{K_n} \in \mathbb{R}^{(K-K_n+1)\times(K+1)}$ is such that $\mathbf{M}_{K_n}\mathbf{s}_n[k] = \operatorname{col}\left(\{s_n[l \mid k]\}_{l\in\mathbb{Z}_{[K_n,K]}}\right)$. ■

In what follows, we refer to Prob. III.1 as the *primal load scheduling problem*. It is obtained by reformulating constraints (9)–(11) and objective (13) in terms of control sequences $\boldsymbol{\pi}_n[k]$ only. This is achieved by eliminating state predictions $\mathbf{T}_n[k]$ and $\mathbf{s}_n[k]$ using (6)–(7) and (12).

IV. Incentive-based Coordinated Charging

In what follows, we derive an iterative, price-coordinated implementation of Prob. III.1. Close inspection of (14) reveals that except for the complicating temperature constraint, i.e., (14b), the centralized charging problem is fully separable in local control sequences $\boldsymbol{\pi}_n$. Thus, if it was not for the temperature constraint that couples the profiles $\boldsymbol{\pi}_n$ for all $n \in \mathcal{N}$, it would be possible to find the optimizer of Prob. III.1 by solving, in parallel, a set of N local PEV-specific optimization problems in $\boldsymbol{\pi}_n$. To derive a non-centralized implementation while still accounting for the coupling temperature constraint, consider the partial dual of Prob. III.1 obtained by relaxing (14b), i.e.,

$$\max_{\boldsymbol{\lambda}\in\mathbb{R}_+^{K+1}} \Upsilon(\boldsymbol{\lambda}) \tag{15}$$

where

$$\Upsilon(\boldsymbol{\lambda}) := \min_{\boldsymbol{\pi}_n \in \Pi_n\left(s_n[0|k]\right)} \sum_{n\in\mathcal{N}} \left(\hat{J}_n(\boldsymbol{\pi}_n) + \boldsymbol{\lambda}^\top \boldsymbol{\Psi}\boldsymbol{\pi}_n\right) + \boldsymbol{\lambda}^\top\left(\boldsymbol{\Phi}\Delta T[0\,|\,k] + \boldsymbol{\Psi}_{\mathrm{d}}\hat{\mathbf{d}} - T_{\max}\mathbf{1}_{K+1}\right),$$

with $\Pi_n\left(s_n[0\,|\,k]\right) := \{\boldsymbol{\pi}_n \in \mathbb{R}^K \;\mid\; \text{(14c)–(14e) holds}\}$,

$$\hat{J}_n(\boldsymbol{\pi}_n) := \boldsymbol{\pi}_n^\top(\boldsymbol{\Psi}_{S_n}^\top \mathcal{Q}_{s,n}\boldsymbol{\Psi}_{S_n} + \mathcal{R}_n)\boldsymbol{\pi}_n + 2(\boldsymbol{\Phi}_{S_n} s_n[0\,|\,k] - \mathbf{1}_{K+1})^\top \mathcal{Q}_{s,n}\boldsymbol{\Psi}_{S_n}\boldsymbol{\pi}_n,$$

and where $\boldsymbol{\lambda} \in \mathbb{R}_+^{K+1}$ is the Lagrangian multiplier or *pseudo-price vector* associated with constraint (14b), see [9].

A well-known decomposition technique from convex optimization, the dual-ascent method, can now be applied to solve Prob. III.1 in a distributed way, see [9], [10]. The underlying observation is that $\Upsilon(\boldsymbol{\lambda})$ allows for separate optimization over $\boldsymbol{\pi}_n, n \in \mathcal{N}$, yielding the following problem.

Problem IV.1 (Open-loop Coordinated PEV Charging) At iteration $p \in \mathbb{Z}_+$, given $s_n[0 \mid k] = s_n[k]$, $\Delta T[0 \mid k] = \Delta T[k]$, disturbance forecast $\hat{\mathbf{d}}[k]$ and price vector $\boldsymbol{\lambda}^{(p)}[k] \in \mathbb{R}_+^{K+1}$, solve for each PEV $n \in \mathcal{N}$,

$$\boldsymbol{\pi}_n^{(p)}[k] = \underset{\boldsymbol{\pi}_n \in \Pi_n\left(s_n[0|k]\right)}{\arg\min} \; \hat{J}_n\left(\boldsymbol{\pi}_n\right) + \left(\boldsymbol{\lambda}^{(p)}[k]\right)^\top \boldsymbol{\Psi}\boldsymbol{\pi}_n. \quad (16)$$

Then, given initial price $\boldsymbol{\lambda}^{(0)}[k]$, generate $\boldsymbol{\lambda}^{(p+1)}[k]$ via

$$\boldsymbol{\lambda}^{(p+1)}[k] = \left[\boldsymbol{\lambda}^{(p)}[k] + \alpha^{(p)}\left(\nabla_{\boldsymbol{\lambda}}\Upsilon\right)\right]_+, \quad (17)$$

with

$$\nabla_{\boldsymbol{\lambda}}\Upsilon := \boldsymbol{\Phi}\Delta T[0 \mid k] + \boldsymbol{\Psi}\left(\sum_{n\in\mathcal{N}} \boldsymbol{\pi}_n^{(p)}[k]\right) + \boldsymbol{\Psi}_{\mathrm{d}}\hat{\mathbf{d}}[k] - T_{\max}\mathbf{1}_{K+1}$$

and iteration-dependent step-size parameter $\alpha^{(p)} \in \mathbb{R}_+$. ■

Prob. IV.1 can be interpreted as follows, see Fig. 2. To decentralize Prob. III.1, we employ a centralized coordinator that is responsible for secure transformer operation, and that supplies the vehicles with a common time-varying pseudo-price for electrical energy, i.e., $\boldsymbol{\lambda}^{(p)}$ [\$/J]. Each PEV owner can respond autonomously to this price. In accordance with (16), rational car owners will adjust their scheduled power demand in a way that complies with their local constraints and minimizes the sum of local objectives (i.e., $\hat{J}_n(\boldsymbol{\pi}_n)$) and energy costs (i.e., $\left(\boldsymbol{\lambda}^{(p)}\right)^\top \Psi\boldsymbol{\pi}_n$). The coordinator is informed about the individual optimal power profiles $\boldsymbol{\pi}_n^{(p)}$ and updates the price in a way that supports feasibility of temperature constraint (14b) at iteration $p+1$. More specifically, the corresponding *master problem*, i.e., maximizing over $\boldsymbol{\lambda}$ in (15), is solved via the *projected subgradient method* using (17). Accordingly, the price is driven towards zero at time instants for which the temperature associated with the profiles $\boldsymbol{\pi}_n^{(p)}$ is predicted to be below $T_{\max}$. However, the price is increased, and thus, charging is discouraged, at instants for which the demand response $\sum_{n\in\mathcal{N}} \boldsymbol{\pi}_n^{(p)}$ would lead to a violation of constraint (9).

Now consider the following theorem.

Theorem IV.2 *Let $\{\alpha^{(p)}\}_{p\in\mathbb{Z}_+}$ with $\alpha^{(p)} \in \mathbb{R}_+$ for $p \in \mathbb{Z}_+$ be such that $\sum_{p=0}^{\infty}\alpha^{(p)} = \infty$ and $\sum_{p=0}^{\infty}\left(\alpha^{(p)}\right)^2 < \infty$. Then the profiles $\boldsymbol{\pi}_n^{(p)}$, $n \in \mathcal{N}$, generated by Prob. IV.1 asymptotically converge to the optimizers $\boldsymbol{\pi}_n^*$ of Prob. III.1, i.e., $\|\boldsymbol{\pi}_n^{(p)} - \boldsymbol{\pi}_n^*\|_2 \to 0$ for $p \to \infty$.*

The above result can be obtained along the following lines. For the above conditions on the step-size sequence $\{\alpha^{(p)}\}_{p\in\mathbb{Z}_+}$, the iterates generated by projected subgradient step (17) are guaranteed to converge asymptotically to the optimizer $\boldsymbol{\lambda}^*$ of (15), see [9], [10]. Thus, Prob. IV.1 asymptotically recovers the optimal Lagrangian multiplier associated with complicating constraint (14b) in Prob. III.1. The result now follows from strong duality of Prob. III.1.

In conclusion, we have obtained a distributed implementation of Prob. IV.1 that allows for autonomous decision making of individual PEV owners based on a common pseudo-price signal. Next, we describe how this incentive-based scheduling problem can be embedded in a model predictive control scheme as a means to provide feedback to disturbances and changing network conditions.

A. Implementation: receding horizon control

The previously defined PEV-load scheduling schemes, i.e., Prob. III.1 and Prob. IV.1, compute an optimal charging profile given a single state measurement and disturbance forecast. Such approaches are only effective if the future temperature and SOC values can be predicted with high accuracy. Although net inelastic demand can be predicted relatively well on the transmission-network level (in an empirical fashion), unexpected fluctuations in background demand can be significant in distribution networks due to a low extent of aggregation. Moreover, for a PEV-load control scheme to be useful, it should allow for varying numbers of connected cars during the charging period. Thus, in practice, it is difficult to avoid significant prediction errors over a long horizon K using open-loop scheduling only. However, we can introduce feedback as a solution to unexpected disturbances, modeling errors and changing numbers of PEVs, by running Probs. IV.1 and III.1 in a receding horizon fashion. This yields a predictive control law that solves the PEV-load scheduling problem each sampling time, while taking a new state measurement and disturbance forecast into account. At each instant $k \in \mathbb{Z}_+$, the first sample of the last obtained control sequences $\boldsymbol{\pi}_n^{(p)}[k]$ is applied to the system, before running the procedure again at time instant $k+1$. This procedure is summarized below.

Algorithm IV.3 *At each time instant $k \in \mathbb{Z}_+$:*
1: *Obtain SOC $s_n[k]$ (PEV controller n), temperature $\Delta T[k]$ and disturbance forecast $\hat{\mathbf{d}}[k]$ (coordinator);*
2: *Initialize $\boldsymbol{\lambda}^{(0)}[k]$ and run Prob. IV.1 for $p_{\max}$ iterations;*
3: *Vehicle n charges its battery at a rate of $\pi_n^{(p_{\max})}[0 \mid k]$.* ■

Fig. 2 depicts the control/communication architecture associated with Alg. IV.3. Red lines represent exchange of information; measurements and physical inputs are reflected by black

lines. The coordinator performs both price update (17) and disturbance estimation, whereas PEV behavior is determined by charging laws (16) and SOC dynamics (2).

In general, there is no guarantee that the iterates $\boldsymbol{\pi}_n^{(p)}$ generated by Prob. IV.1 will be feasible for $p < \infty$. However, in practice, it may still be possible to obtain a feasible (yet, not necessarily optimal) set of PEV charging schedules within a finite number of iterations. In what follows, we assume that $p_{\max} < \infty$ iterations are sufficient for this to occur. Then, for Alg. IV.3 to be suited for implementation in practice, it is necessary that the time required for evaluating these iterations does not exceed the sampling period T_s.

Simulation results (see Sect. V) indicate that the number of iterations required for obtaining feasible control actions may be reduced by appropriately choosing the sequence $\{\alpha^{(p)}\}_{p\in\mathbb{Z}_+}$. Also, convergence speed may be increased considerably in case of small prediction errors, by initializing $\boldsymbol{\lambda}^{(0)}[k] = \{\lambda^{(0)}[l \mid k]\}_{l\in\mathbb{Z}_{[0,K]}}$ as a time-shifted version of the previous price $\boldsymbol{\lambda}^{(p_{\max})}[k-1]$, i.e., $\lambda^{(0)}[l \mid k] := \lambda^{(p_{\max})}[l+1 \mid k-1]$, $l \in \mathbb{Z}_{[0,K-1]}$, and random $\lambda^{(0)}[K \mid k] \in \mathbb{R}_+$, for $k \in \mathbb{Z}_{\geq 1}$. Yet, to the best of our knowledge, general results on the convergence rate of dual-ascent based optimization schemes are lacking still.

Remark IV.4 In Alg. IV.3, Prob. IV.1 is run for $p_{\max}$ iterations each sampling instant. To avoid superfluous computations and reduce the extent of communication between the vehicles and the coordinator, it may be attractive to stop iterating earlier, based on some convergence test criterion. For example, if the convergence of $\boldsymbol{\lambda}^{(p)}$ is monotonic and super-linear, sufficiently accurate approximation of $\boldsymbol{\lambda}^*$ can be concluded if $\|\boldsymbol{\lambda}^{(p)} - \boldsymbol{\lambda}^{(p-1)}\| < \varepsilon$ for a small $\varepsilon \in \mathbb{R}_+$.

Although the receding-horizon feedback mechanism in Alg. IV.3 helps to reduce the effects of prediction inaccuracy, robust feasibility can only be guaranteed if some uncertainty model is explicitly accounted for during open-loop scheduling, i.e., in Prob. III.1 or Prob. IV.1. In what follows, we assume that the background demand and ambient temperature can be predicted up to a certain accuracy, that is, $d[l+k] = \hat{d}[l \mid k] + \delta[l+k]$, with arbitrary, unknown $\delta[l+k] \in \Delta \subset \mathbb{R}^2$. One way of establishing robust feasibility of Prob. III.1 with respect to inaccuracies δ in the (compact) set Δ, consists of replacing (14b) by the constraint

$$\boldsymbol{\Phi}\Delta T[0 \mid k] + \boldsymbol{\Psi}\left(\sum_{n\in\mathcal{N}} \boldsymbol{\pi}_n\right) + \boldsymbol{\Psi}_\mathrm{d}\hat{\mathbf{d}} + \begin{bmatrix} \max_{\boldsymbol{\delta}\in\Delta^K} [\boldsymbol{\Psi}_\mathrm{d}\boldsymbol{\delta}]_1 \\ \vdots \\ \max_{\boldsymbol{\delta}\in\Delta^K} [\boldsymbol{\Psi}_\mathrm{d}\boldsymbol{\delta}]_{K+1} \end{bmatrix} \leq T_{\max}\mathbf{1}_{K+1}, \quad (18)$$

A similar worst-case feasibility approach can be employed in Prob. IV.1, by appropriate modification of $\nabla_{\boldsymbol{\lambda}}\Upsilon$ in (17).

V. Case Study: Overnight PEV Charging

Next, we simulate the charging of $N = 20$ PEVs during an overnight period from 20:00h (i.e., $t = 0\,\mathrm{s}$) to 8:00h. Table I summarizes the simulation scenario, where the bracket notation $[a, b]$, denotes randomly distributed values over the interval $\mathbb{R}_{[a,b]}$. The PEV fleet is heterogeneous in terms of cost parameter values R_n and $Q_{s,n}$, battery parameters η_n and charging rate limits $\pi_{n,\max}$; the latter two were selected to resemble those of today's PEVs. The ambient temperature T_a is constant and representative for a hot summer night. The employed SOC and charging penalties are constant, except for a factor 10 increase in R_n after time K_n. This reflects that PEV owners prefer to charge quickly early in the evening. The background load $i_\mathrm{d}[k]$, see Fig. 3(c), is representative for the nightly power demand of 100 households. Finally, note that the sequence $\alpha^{(p)}$ satisfies the conditions of Thm. IV.2.

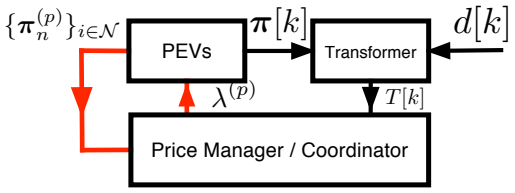

Fig. 2. Control/communication architecture of coordinated PEV control.

TABLE I
Simulation Parameters

Parameter	Value	Unit
Sampling Time, T_s	155	s
Temperature limit, $T_{\max} + T^*$	393	K
Ambient temperature, $T_a[k]$	303	K
Initial temperature, $T[0]$	333	K
Transformer parameters, τ, ρ, γ	0.9, 0.1, 0.85	-, -, K/A
Battery parameter, η_n	[0.47, 0.75]	1/kA
Current bounds, $\pi_{n,\min}$, $\pi_{n,\max}$	0, [10, 20]	A
Initial SOC, $s_n[0]$	[0, 0.2]	-
Required minimum SOC, S_n	[0.8 1.0]	-
Required minimum SOC time, K_n	[4:00, 8:00]	hr:min
Initial control input penalty, R_n	[0.05, 0.10]	-
State penalty, $Q_{s,n}$	[10, 20]	-
Dual-ascent step-size parameter, $\alpha^{(p)}$	$2/\lceil p/3 \rceil$	1 / K
Iterations per time instant, $p_{\max}[k]$	150 to 20	iterations

We evaluated the performance of Prob. III.1 and Prob. IV.1 in closed-loop with the *linearized* system characterized by Table I and (2), (5). Additionally, we simulated uncoordinated charging by evaluating Prob. IV.1 for an all-zero price signal, i.e., $\boldsymbol{\lambda}^{(p)}[k] = \{0, \ldots, 0\}$, for all $k, p \in \mathbb{Z}_+$. All schemes were implemented in a receding horizon fashion, using a 12 h prediction horizon at time instants between 20:00h and 22:00h, and a shrinking horizon with a fixed end-point at 10:00h at time instants after 22:00h. The coordinator was provided with a perfect forecast of $T_a[t]$ and a 5 % uncertain forecast of demand $i_d[k]$, i.e., $i_d[l+k] = \hat{i}_d[l \mid k] + \delta_i[l+k]$ with $\delta_i[k] \in \Delta_i[k] := \mathbb{R}_{[-0.05\hat{i}_d[k], 0.05\hat{i}_d[k]]}$. Robust feasibility was ensured via temperature constraint (18).

Fig. 3 shows the simulation results for the three charging schemes. Clearly, the uncoordinated method performs poorly, since, without the price signal, the PEVs are not affected by the temperature constraint and thus charge rapidly, taking only their own SOC requirements and objectives into account (Fig. 3(b)). Consequently, the temperature exceeds $T_{\max}$ for over 3 hours, which could result in transformer failure.

In contrast to uncoordinated charging, both Prob. III.1 and Prob. IV.1 respected temperature constraint (9). Note that the

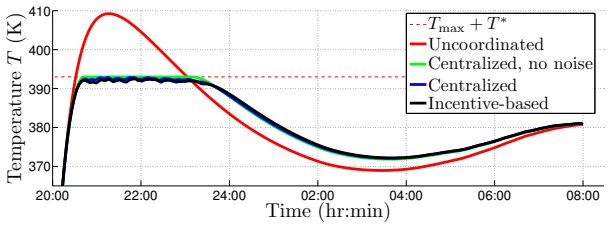

(a) Transformer temperature $T[k]$.

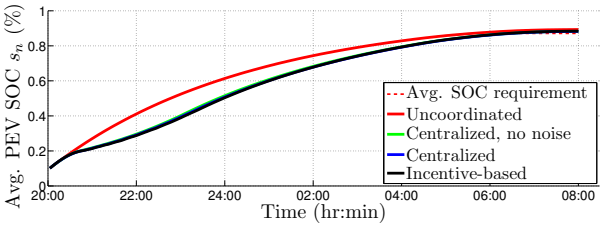

(b) Average SOC target $\text{avg}(S_n)$ and profiles $\text{avg}(s_n[k])$.

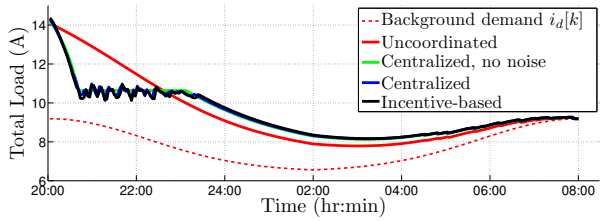

(c) Aggregated transformer current $\pi[k] + i_{\text{d}}[k]$.

Fig. 3. Performance of Prob. III.1, Prob. IV.1, and uncoordinated charging.

uncertainty margin employed in (18) caused a performance degradation of less than two degrees Kelvin as compared to the noise-free centralized scheme. Also, observe that the noisy coordinated incentive-based scheme and the noisy centralized scheme induce only slightly different current and temperature trajectories, despite $p_{\max}$ being finite.

Because the employed cost functions (13) (and, equivalently, (16)) heavily penalize non-fully charged batteries early in the evening, PEV owners attempt to charge as quickly as possible. Fig. 3(a) shows that as a result, the temperature reaches $T_{\max}$ as soon as ca. 8:30h. In response to this, the coordinator increases the price to suppress charging (Fig. 4), and thus, overloading is prevented. In response to the decrease in price that occurs from 21:00h to 23:30h, the PEV charging current increases again. After 00:00h, the increased penalty on control effort comes with a reduced priority for rapid charging, causing the average charging rate to decrease slightly. Combined with low inelastic demand, this causes the transformer temperature to drop below $T_{\max}$, and thus, the optimal price $\lambda^*[k]$ is driven to zero (in accordance with complementary slackness of the optimal Lagrangian multiplier [9]). For the remainder of the night, the network offers plenty of charging capacity and the PEV owners can charge freely, unhindered by a non-zero price, to reach their SOC target while minimizing their local objectives.

Moreover, even though we employed finite $p_{\max}$ and a 5% uncertain load forecast, the incentive-based control scheme performed nearly optimal and was feasible with respect to constraints (8)-(11) at all simulated time instants.

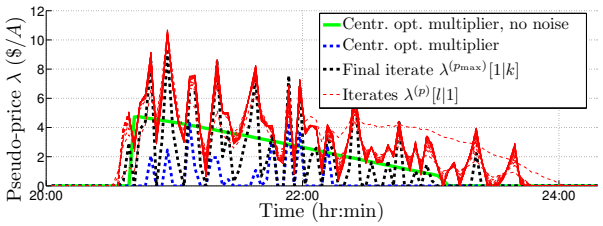

Fig. 4. Convergence of the incentive-based charging scheme for $k = 0$.

VI. Conclusions

Simultaneous overnight charging of plug-in electric vehicles (PEVs) may cause severe overloading of substation transformers in the near future. A distributed incentive-based demand-scheduling problem was derived as a solution to this issue, based on a dynamical model of a small PEV fleet that is served by a single temperature-constrained transformer. Feedback to disturbances was provided by evaluating the open-loop scheduling problem in a receding horizon fashion, yielding an iterative model predictive control (MPC) scheme in which the individual PEVs can autonomously respond to incentives provided by a coordinator that is responsible for secure transformer operation. Simulation results showed that even for a finite number of iterations, the method can be effective in terms of enforcing the temperature constraint.

For real-time implementation, it is key that the PEV coordination scheme can generate feasible control actions within each sampling period. Future work will therefore focus on improving the convergence rate of the iterative scheduling problem, and alternative non-centralized implementations that may exhibit faster convergence will be investigated.

References

[1] P. Fairley, "Speed bumps ahead for electric-vehicle charging," *IEEE Spectrum*, vol. 47, no. 1, pp. 13–14, January 2010.

[2] L. Kelly, A. Rowe, and P. Wild, "Analyzing the impacts of plug-in electric vehicles on distribution networks in British Columbia," in *IEEE Electrical Power & Energy Conference*, Montréal, QC, Canada, October 2009.

[3] Z. Ma and D. Callaway, "Optimal centralized charging of large populations of plug-in electric vehicles," Tech. Rep., June 2010.

[4] K. Clement-Nyns, E. Haesen, and J. Driesen, "The impact of charging plug-in hybrid electric vehicles on a residential distribution grid," *IEEE Transactions on Power Systems*, vol. 25, no. 1, pp. 371–380, March 2010.

[5] E. Sortomme, M. M. Hindi, S. D. J. MacPherson, and S. S. Venkata, "Coordinated charging of plug-in hybrid electric vehicles to minimize distribution system losses," *IEEE Transactions on Smart Grid*, vol. 2, no. 1, pp. 198–205, Dec 2011.

[6] M. D. Galus, R. A. Waraich, and G. Andersson, "Predictive, distributed, hierarchical charging control of PHEVs in the distribution system of a large urban area incorporating a multi agent transportation simulation," in *Power Systems Computation Conference*, Stockholm, Sweden, August 2011.

[7] Z. Ma, D. Callaway, and I. Hiskens, "Decentralized charging control for large populations of plug-in electric vehicles," *IEEE Transactions on Control Systems Technology*, (to appear).

[8] L. Gan, U. Topcu, and S. Low, "Optimal decentralized protocol for electric vehicle charging," in *50th IEEE Conference on Decision and Control*, Orlando, FL, USA, December 2011.

[9] D. P. Bertsekas, *Nonlinear Programming*. Belmont, MA, USA: Athena Scientific, 1999.

[10] N. Z. Shor, *Minimization methods for nondifferentiable functions*. Berlin: Springer, 1985, translated from Russian.